Supporting Information

Revealing Interfacial Parasitic Reactions of Nitrile Rubber Binders in All-Solid-State Lithium Batteries

Jaecheol Choi, Ju Young Kim, Seok Hun Kang, Dong Ok Shin, Myeong Ju Lee, Young-Gi Lee**

1. Experimental Section

Materials: The commercial nitrile butadiene rubber (NBR, Mv ~ 80k, nitrile content ~ 32%) and polybutadiene (PB, Mw ~200k) were supplied by LG Chem and Sigma aldrich korea, respectively and used without any purification. $LiNbO_3$-coated $LiCoO_2$ and $LiNbO_3$-coated $LiNi_{0.6}Co_{0.2}Mn_{0.2}O_2$ were purchased from NEI corporation in USA. Li_6PS_5Cl (LPSCl, average particle size ~ 3um, ionic conductivity ~ 3 mS cm^{-1}) was purchased from Posco JK Solid Solution in Korea. Super P Li® was purchased by Imerys in Switzerland. Anisole solvent and Lithium metal (Thickness ~300 um) were purchased by Sigma-Aldrich and Honjo metal in Japan, repectively. It is important to note that all chemicals used in this work are consistently stored in a dry room where the dew point was maintained consistently below -60 °C. Consequently, any moisture absorbed/adsorbed on the chemicals is likely to desorb before use.

Preparation of sheet-type $LiCoO_2$ composite electrode: The LCO cathode slurry was prepared by mixing 60 wt.% $LiCoO_2$, 35 wt.% LPSCl, 3 wt.% Super P Li®, and 2 wt.% NBR (or PB) dissolved in anisole with a planatery mixer (Thinky corp., ARM-310). Electrode composition was slightly changed for the case of control experiments and the changes were mentioned in the manuscipt. The viscosity of slurry was adjusted by additional anisole and homogeneously dispersed slurry was obtained. The prepared slurry was subsequently coated onto Ni foil (10

μm, Nipon steel, Japan) and dried in a convection oven at 120 °C for 30 min. The mass loading of $LiCoO_2$ was controlled at 7.5 mg cm^{-2}, corresponding to approximately 1.1 mAh cm^{-2} of the areal capacity. All procedures were performed in a dry room with a dew point of -60 °C. In case of mechanistic analysis, LPSCl electrode composed of LPSCl, Super P Li and NBR was prepared without LCO active materials. For the preparation of LPSCl electrode, a same procedure that used for LCO electrode preparation was adopted, but the weight ratio of electrode was fixed to LPSCl/Super P Li/ NBR (or PB) = 95/3/2 (wt%) unless otherwise mentioned.

Cell assembly and evaluation of all solid-state batteries: To prepare a layer of solid electrolyte, ~ 150 mg of LPSCl powder was pelletized in a home-made polyether ether ketone mold using a hydraulic uniaxial press at 450 MPa. $LiCoO_2$ electrode was placed on one side of the pelletized SE layer and cold pressed at 450 MPa and then Li metal was placed on the other side of pelletized SE layer to form a lithium metal half-cell. All cells were tested under constant stacking pressure of 36 MPa. Prior test for electrochemical performance, all cells were sealed with Al pouch to avoid exposure of humid air. For battery evaluation, cells were firstly charged/discharged at 0.1 C in the potential range of 3.0 – 4.2 V for 3 cycles as formation step. After the formation step, the cells were charged and discharged at 0.2 C, 0.5 C, 1.0 C for 3 cycles each to evaluate rate capability, followed by cycle life tested at 1 C for 100 cycles. All cells underwent charging up to 4.2 V using constant current and constant voltage modes, followed by discharging to 3.0 V via constant current mode.

For the analysis of electrochemical behavior, cyclic voltammetric (CV) analysis was performed at a scan rate of 0.2 mV s^{-1} in the same potential range applied for battery test. Impedance analysis was performed using cells after cycling in amplitude of 10 mV between frequencies of 10^{-1} – 10^{6} Hz.

Material characterizations: X-ray photoelectron spectrometry (XPS) spectra on the electrodes composed of NBR, PB binders were confirmed by using XPS spectrometer (ESCALAB 250Xi, Thermo Scientific, USA) for the surface analysis. Peel strength measurement was carried out using a 180o peel test machine with a testing speed of 0.50 mm/s.

2. Supporting Figures and Tables

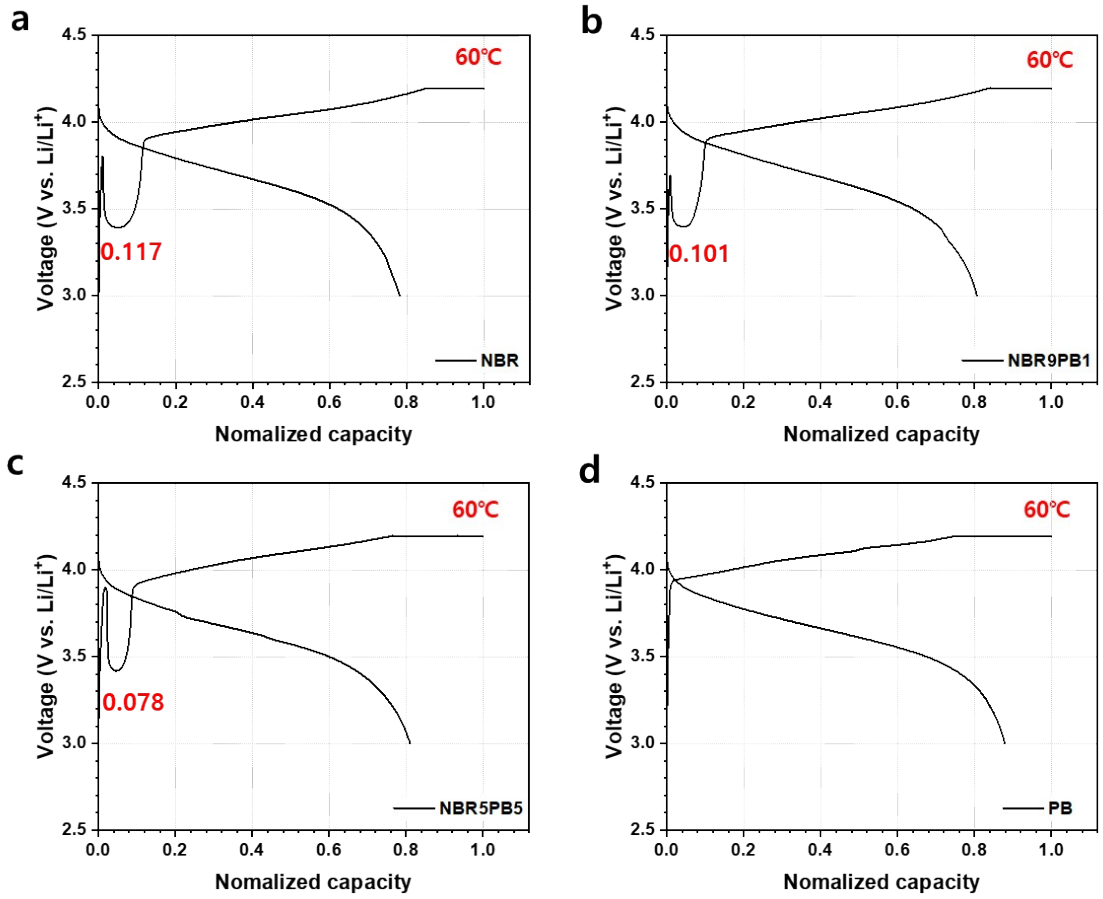

Figure S1. Redrawn voltage profiles obtained from Figure 1a, in which the charge/discharge capacities were normalized with respect to the total charge capacity.

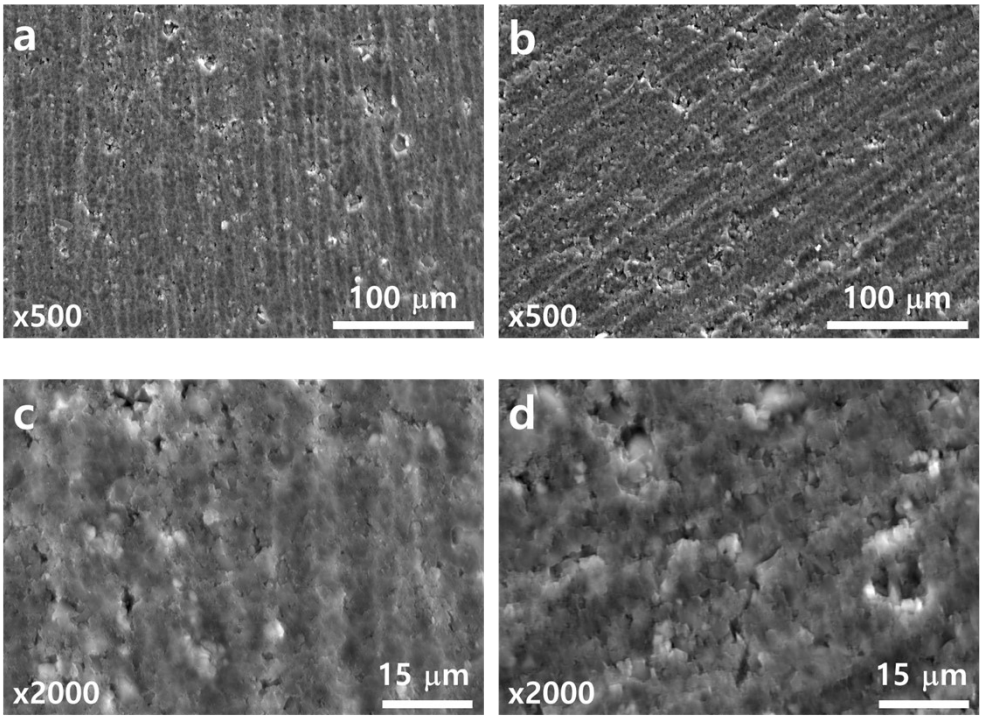

Figure S2. Morphological analysis before and after formation cycle, Low magnificent SEM images of a) before and b) after formation. High magnificent SEM images of c) before and d) after formation.

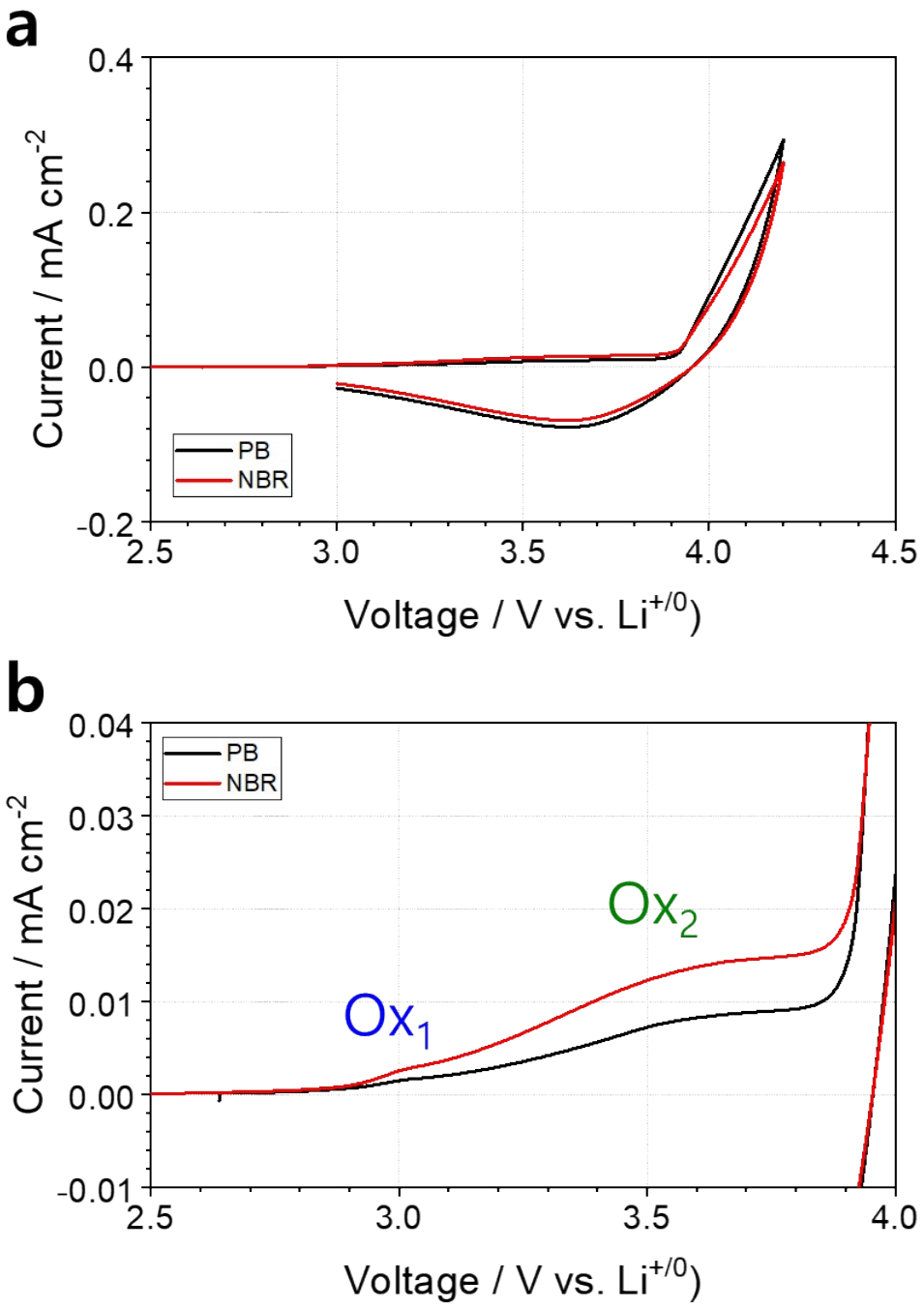

Figure S3. a) Electrochemical behavior of NBR (red) or PB (black) containing LCO electrode measured with a scan rate of 0.2 mV s^{-1} at 25 °C. b) magnified CV profiles of panel a.

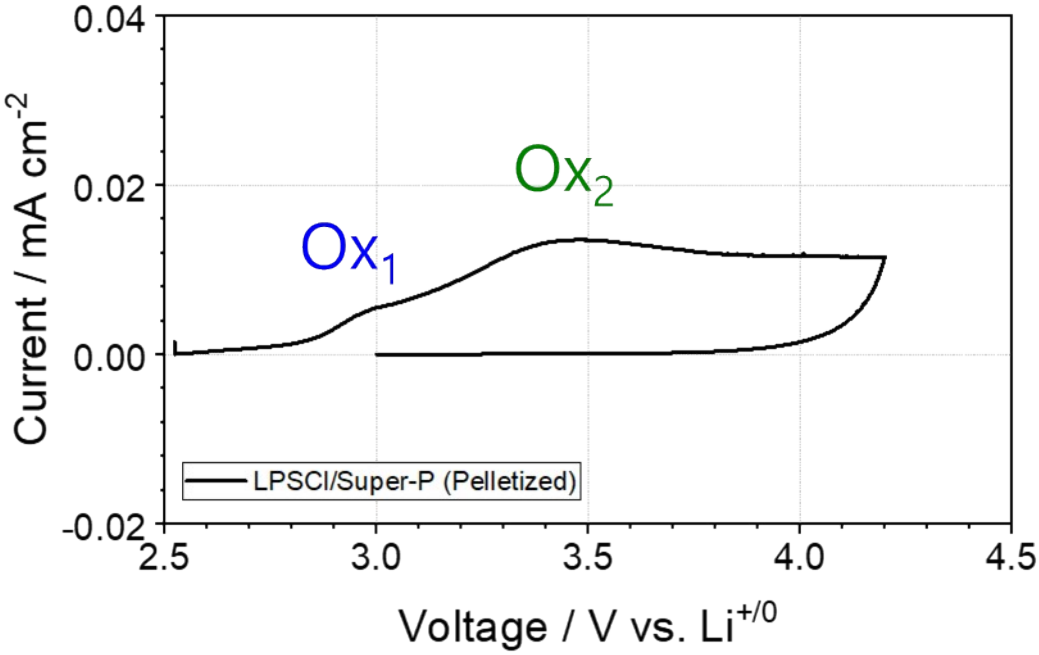

Figure S4. Electrochemical behavior of LPSCl pelletized with 10 wt% conductive carbon at 450 MPa (cell configuration: Li metal (anode), LPSCl pellet (electrolyte layer), LPSCl+Super-P (cathode), costant stacking pressure of 48 MPa)

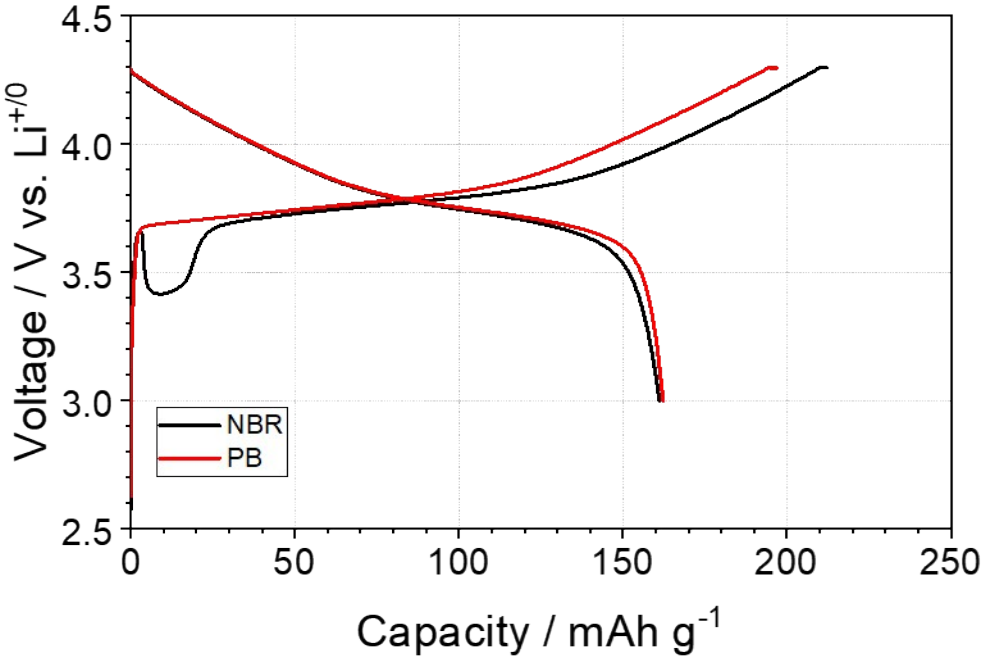

Figure S5. Charge-discharge volate profiles of NCM622 electrode fabricated by the same method used in Figure 1. Only LCO active material was replaced with NCM622 (red line: PB binder, black line: NBR binder).

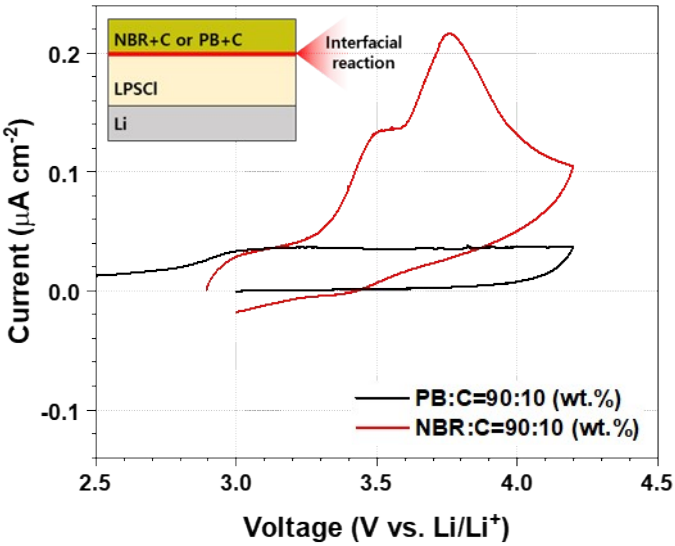

Figure S6. Electrochemical behavior of NBR or PB film composed of 10 wt% conductive carbon. The polymer films were prepared by slurry casting and cold-pressed at 450 MPa prior to assembling the solid-state cells. (cell configuration: Li metal (anode), LPSCl pellet (electrolyte layer), Polymer film (cathode), costant stacking pressure of 48 MPa)

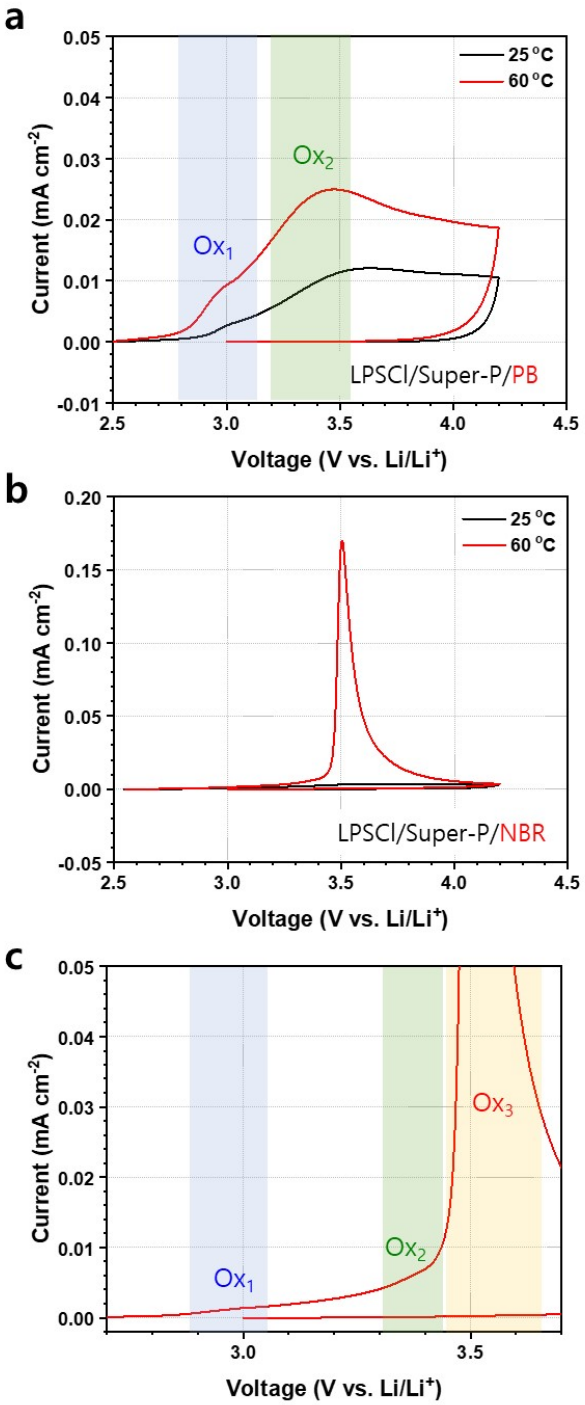

Figure S7. Electrochemical analysis of LPSCl electrodes, composed of conductive carbon and binder a) PB or b) NBR at two different temperatures of 25 °C and 60 °C. c) magnified CV profiles of panel b.

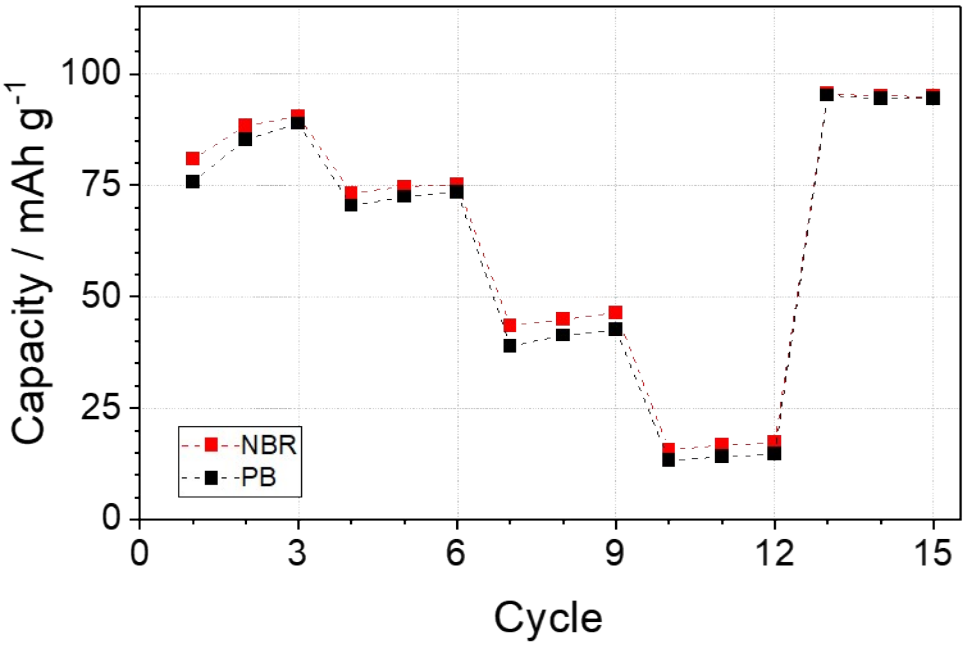

Figure S8. Rate capability test using PB (black) or NBR (red) containing LCO electrode at 25 °C.

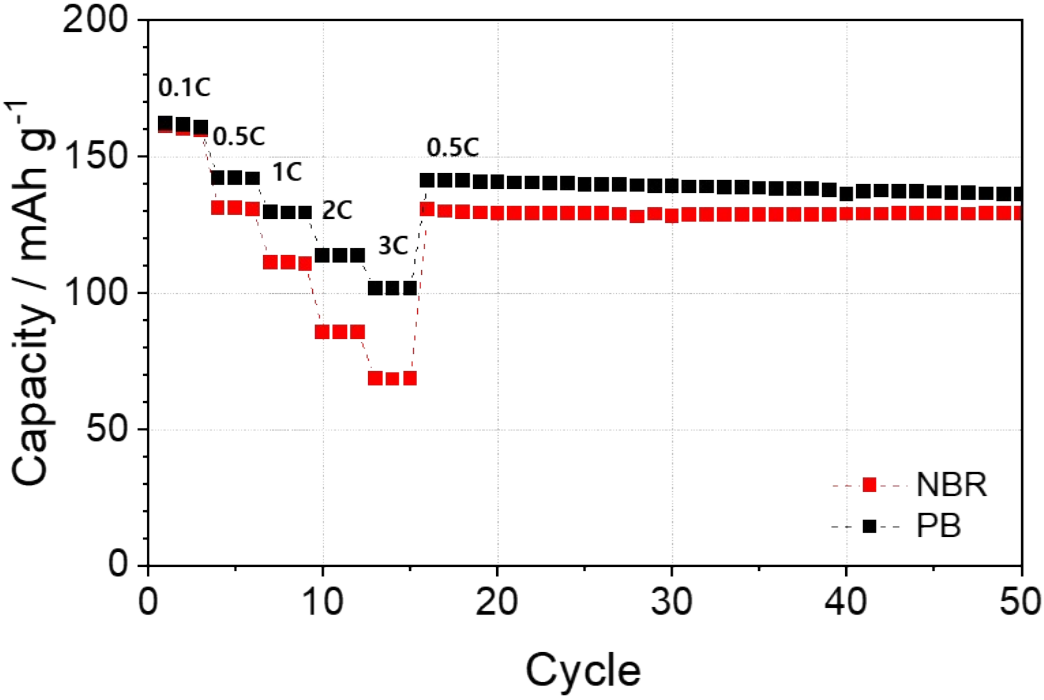

Figure S9. Rate capability and cyclability test using PB (black) or NBR (red) containing NCM622 electrode at 60 °C.

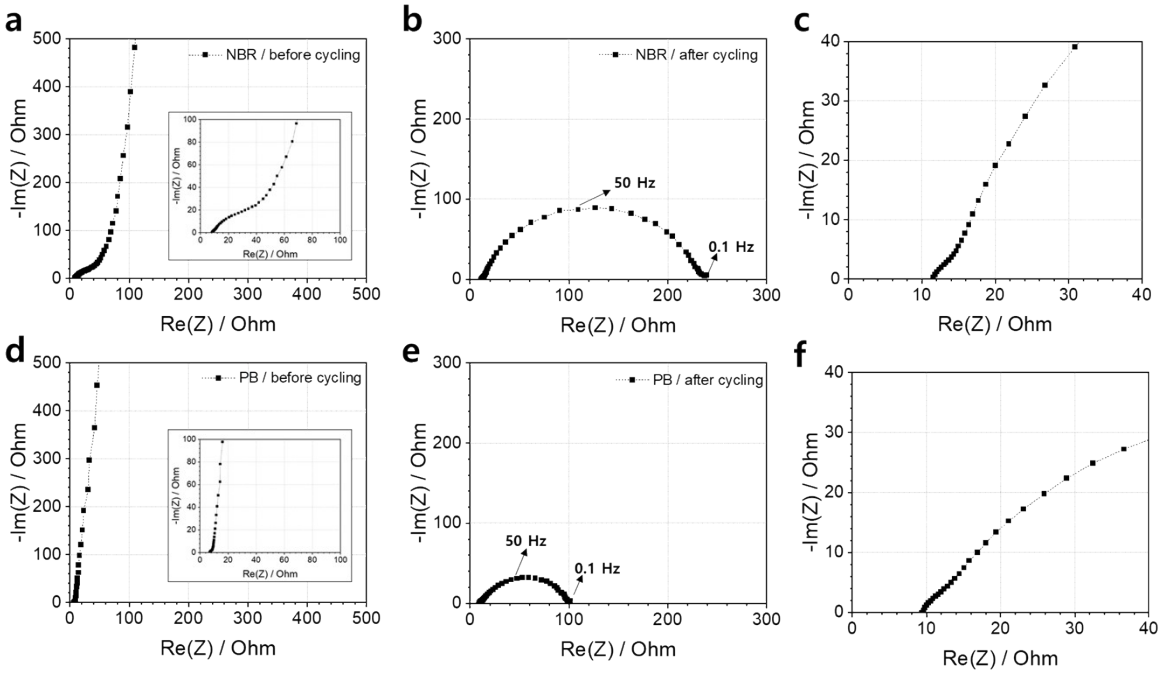

Figure S10. a) Impedance spectra for before cycling for a) NBR and d) PB binder conaining electrode (Inset for bulk resistance of each system) and after cycling for b) NBR and e) PB binder containing electrode. c and f) Enlarged EIS profiles for bulk resistance of panel b and c.

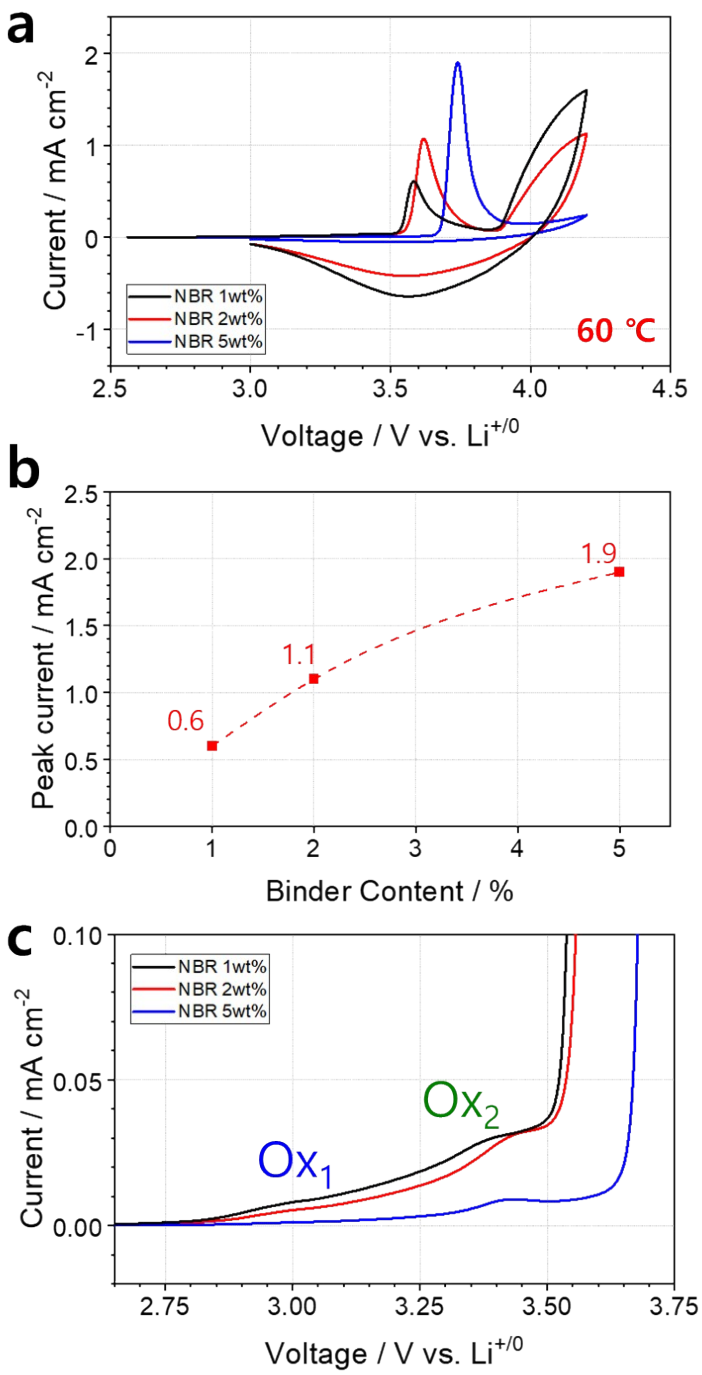

Figure S11. Nitrile content dependence on the side reaction in LCO composite electrode prepared by varying contents of NBR. a) Electrochemical analysis of LCO composite electrodes with 1wt%, 2wt% and 5wt% NBR. b) Quantitified analysis of peak current density as a function of binder content. c) magnified CV profiles of panel a.

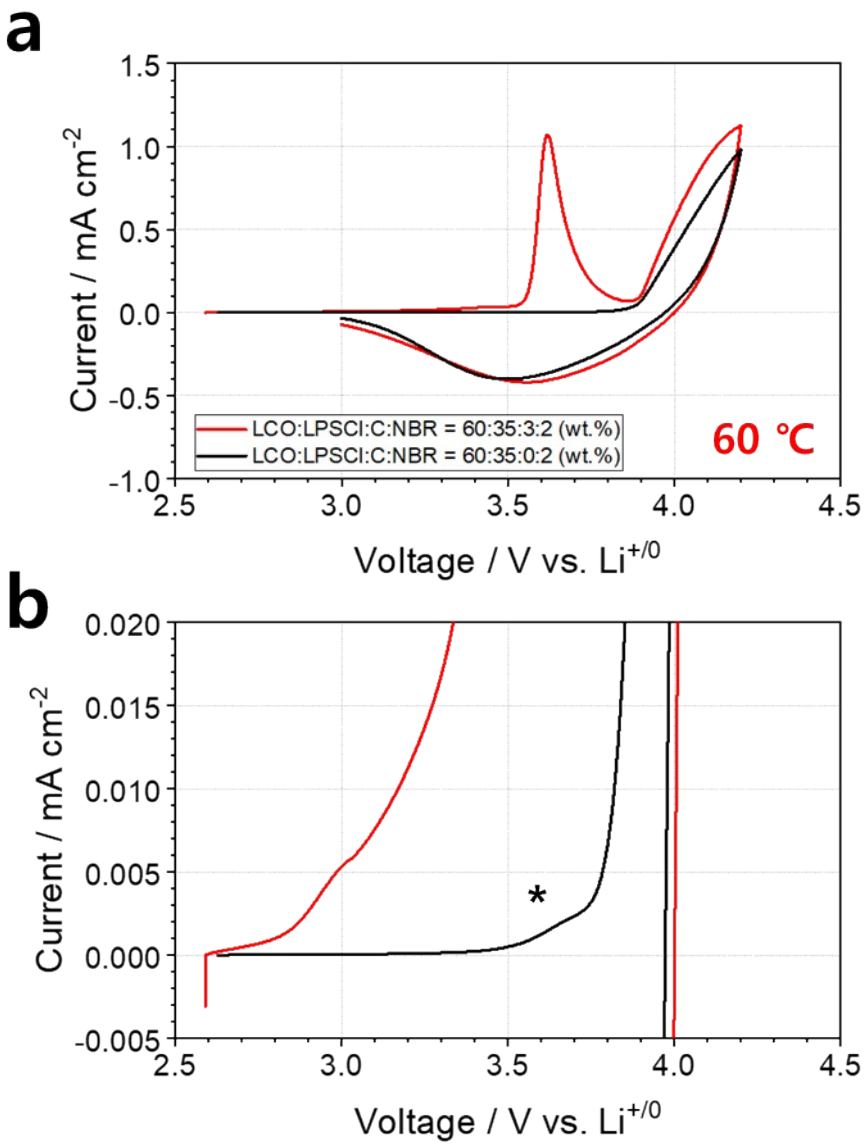

Figure S12. Conductive carbon effects on the LPSCl oxidation and nitrile decomposition. a) Electrochemical analysis of LCO composite electrodes prepared with and without carbon. b) magnified CV profiles of panel a.

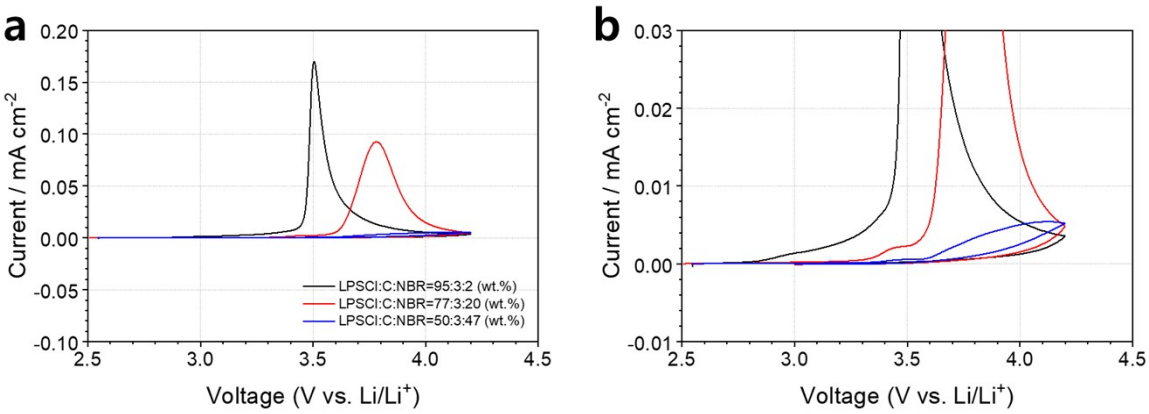

Figure S13. Examination of NBR chemical structure transformation using LPSCl contaning different contents of NBR binder. a) Electrochemical analysis of LPSCl electrodes through cyclic voltammetry and b) magnified CV profiles of panel a.

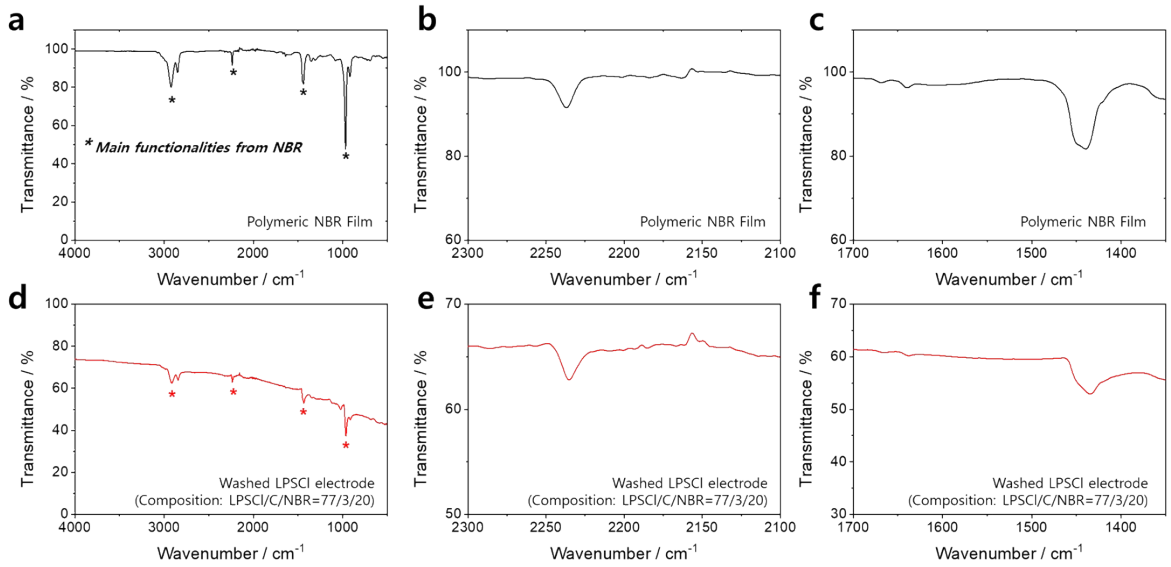

Figure S14. IR spectra comparison. a-c) IR spectra from NBR film electrode and d-f) washed LPSCl electrode (composition – LPSCl/C/NBR=77/3/20, weight %) without electrochemical test.

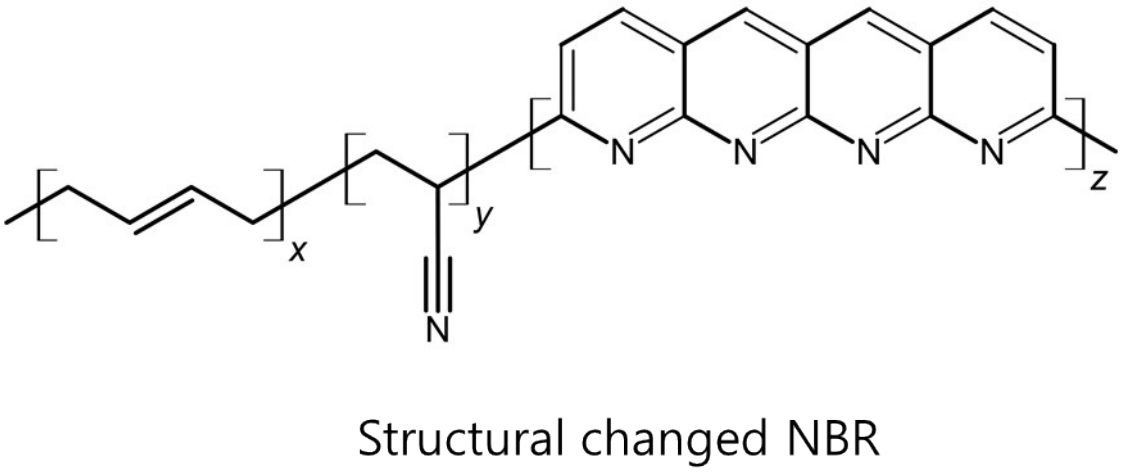

Figure S15. Proposed chemical structure transformation of NBR binder in battery operation and the formation of structural changed NBR.

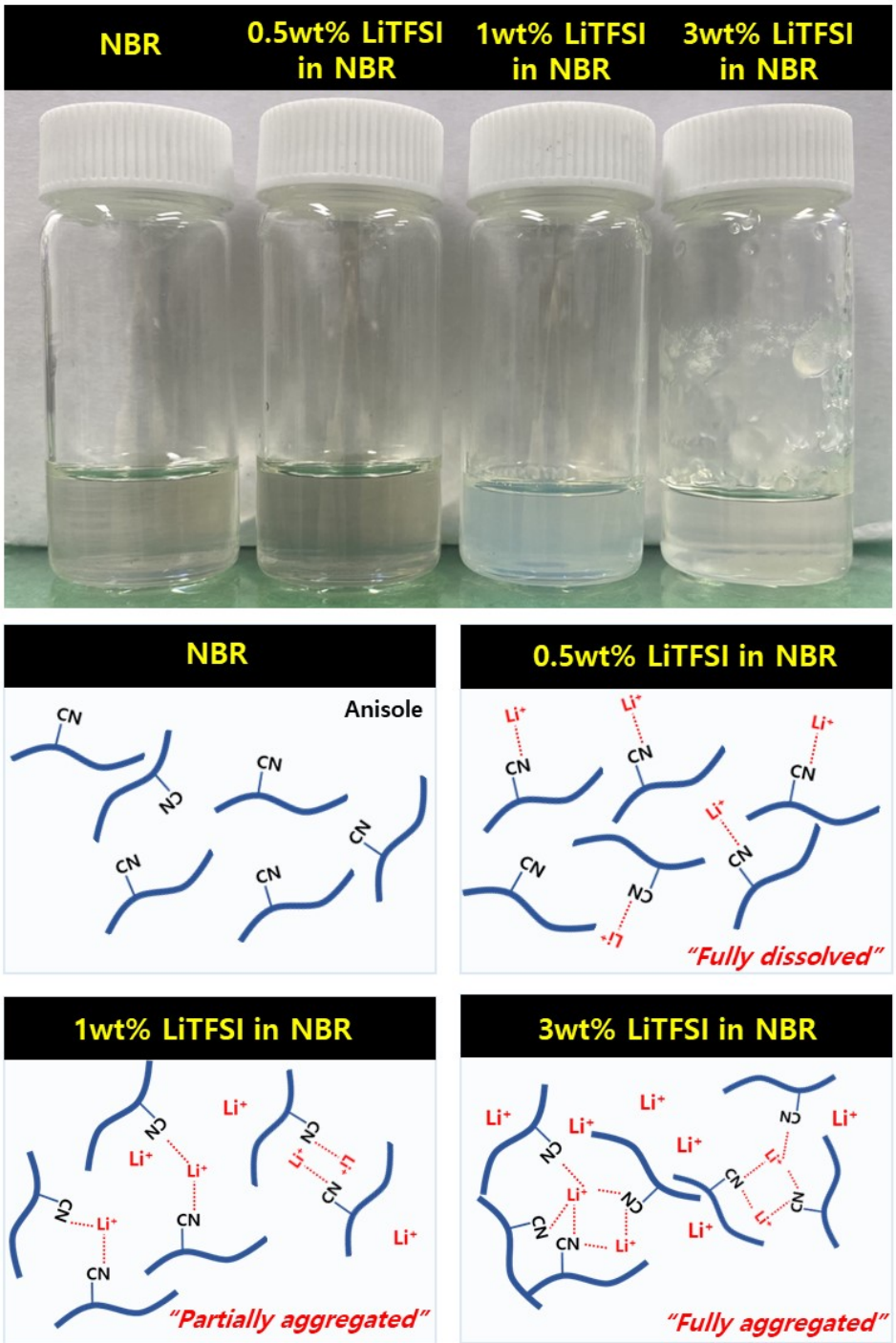

Figure S16. LiNBR preparation with different concentrations of LiTFSI.

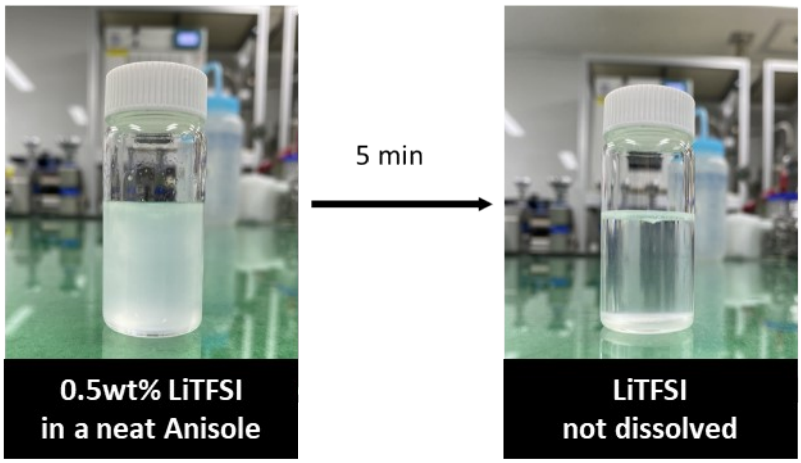

Figure S17. LiTFSI solubility test in neat anisole solvent.

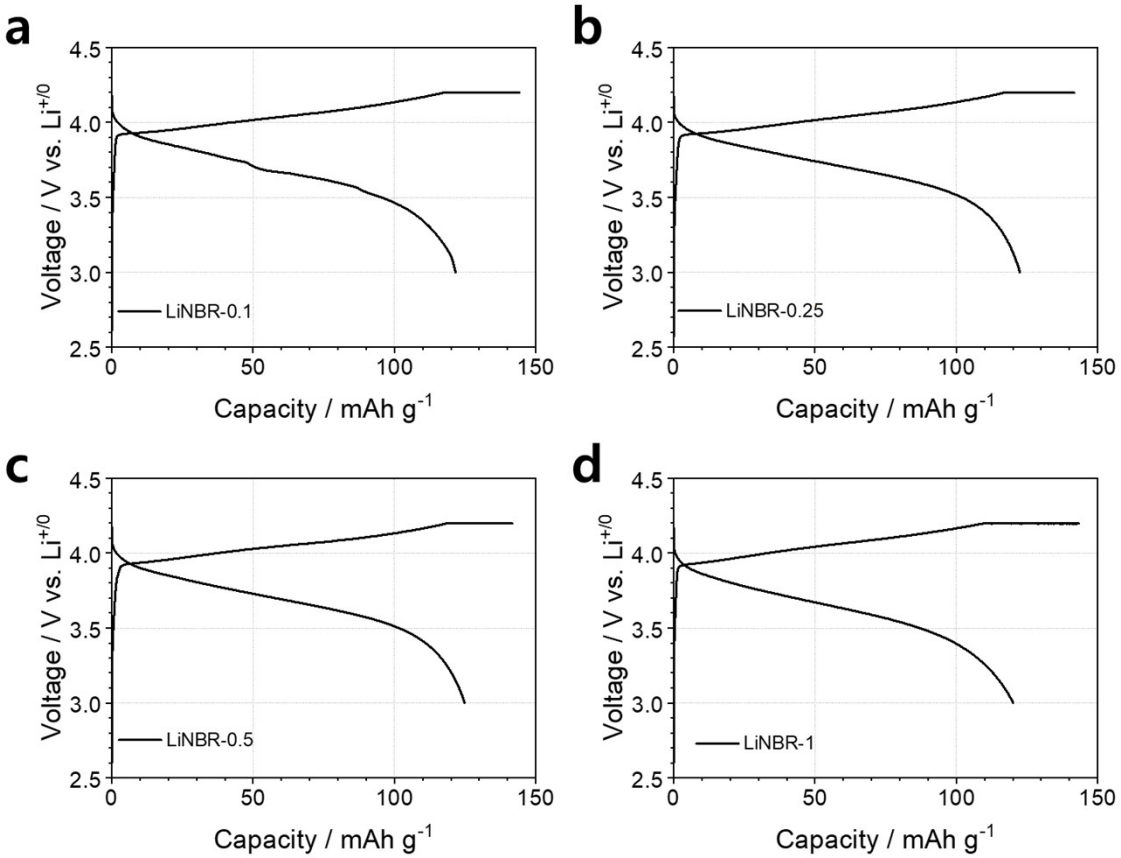

Figure S18. Investigation of Li-salt concentrations in Li-NBR binders on the initial charging-discharging properties. a) LiNBR-0.1wt%, b) LiNBR-0.25wt%, c) LiNBR-0.5wt%, and d) LiNBR-1wt%.

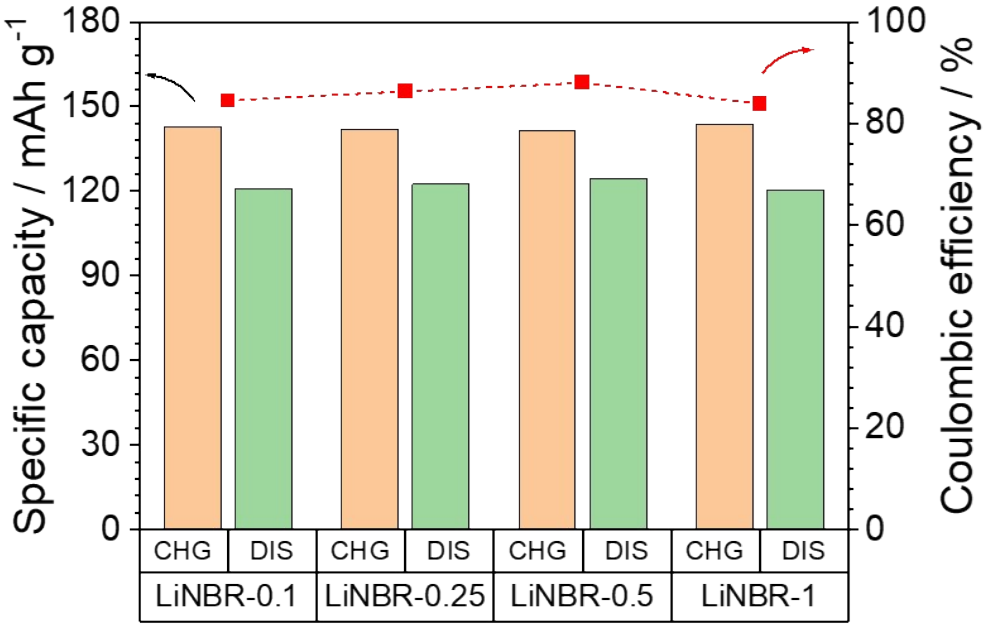

Figure S19. Summary of the first charge/discharge capacity and coulombic efficiency of the LiNBR-x (x= 0.1, 0.25, 0.5, 1 wt%) containing LCO electrode.

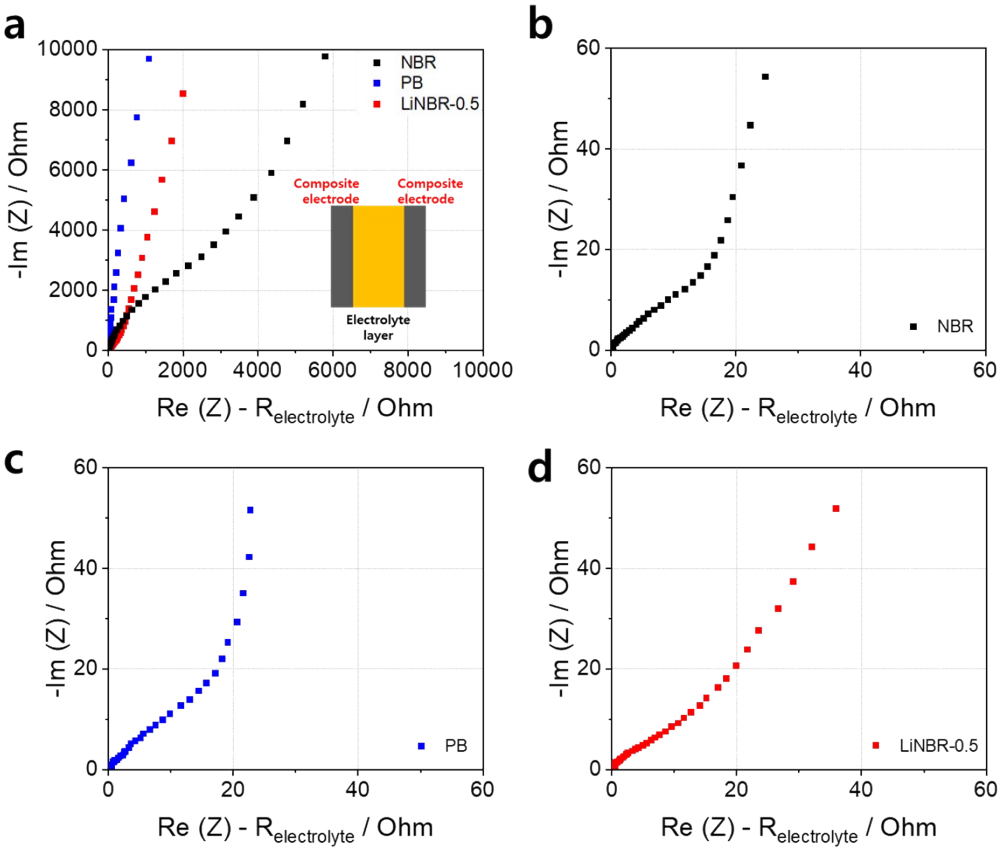

Figure S20. a) Transmission line model results of composite electrodes containing different binders (Inset: cell configuration). b) Enlarged impedance spectrum for NBR electrode. c) Enlarged impedance spectrum for PB electrode. d) Enlarged impedance spectrum for LiNBR-0.5 electrode.

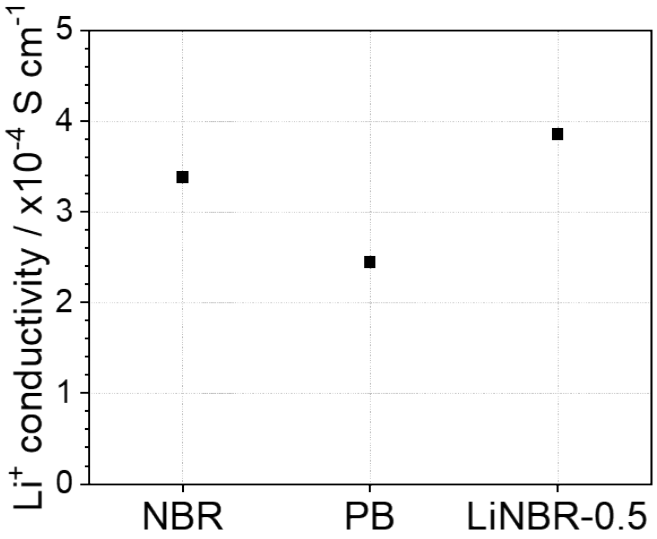

Figure S21. Summary of Li+ conductivity for each binder system.

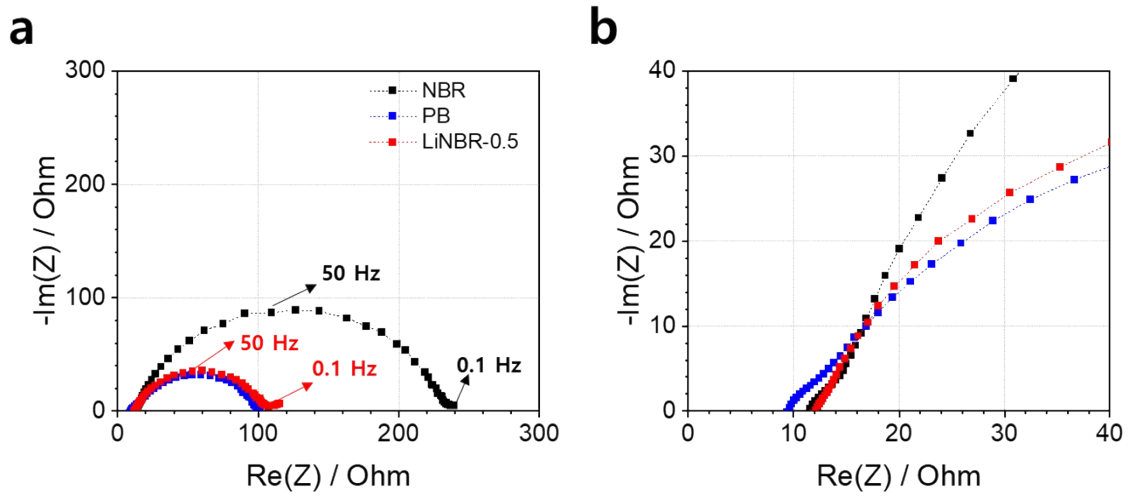

Figure S22. Impedance spectra of NBR (black), PB (blue) or LiNBR (red) containing LCO electrode after evaluation of cyclability for 100 cycles.

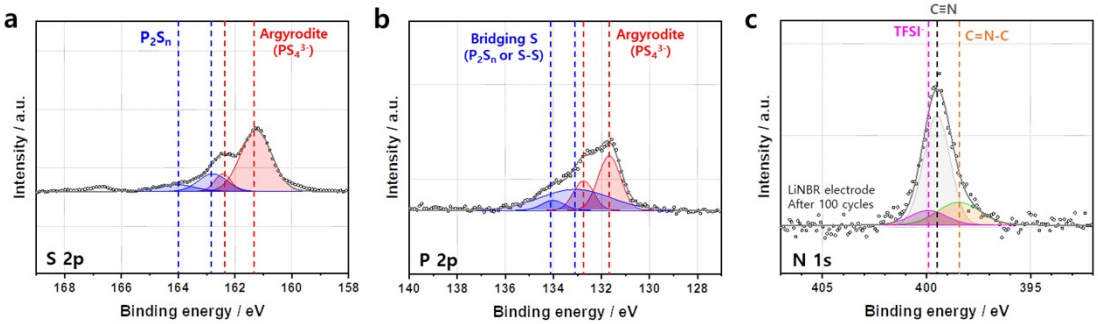

Figure S23. XPS spectra of S 2p, P 2p and N 1s rigion obtained from the LiNBR containing LCO composite electrode after 100 cycles at 60℃

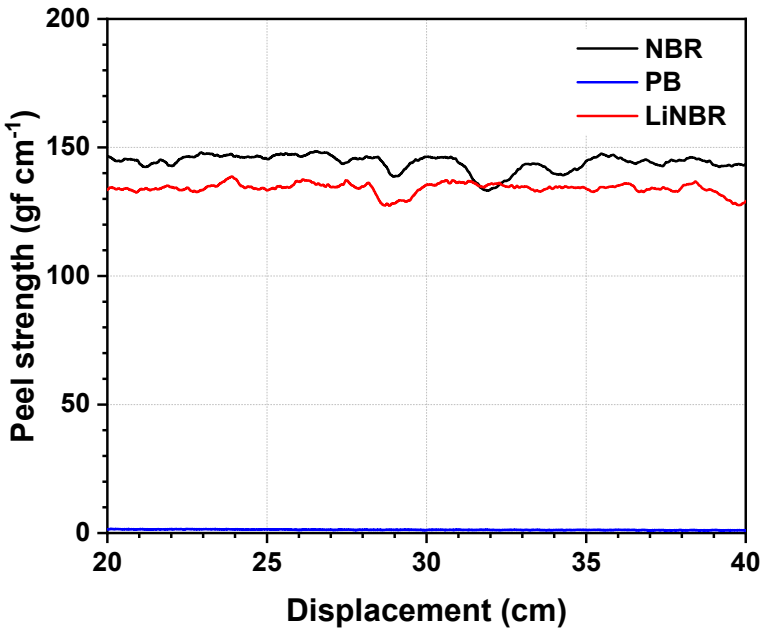

Figure S24. Peel strength measurement with LCO composite electrodes employing NBR, PB or LiNBR.

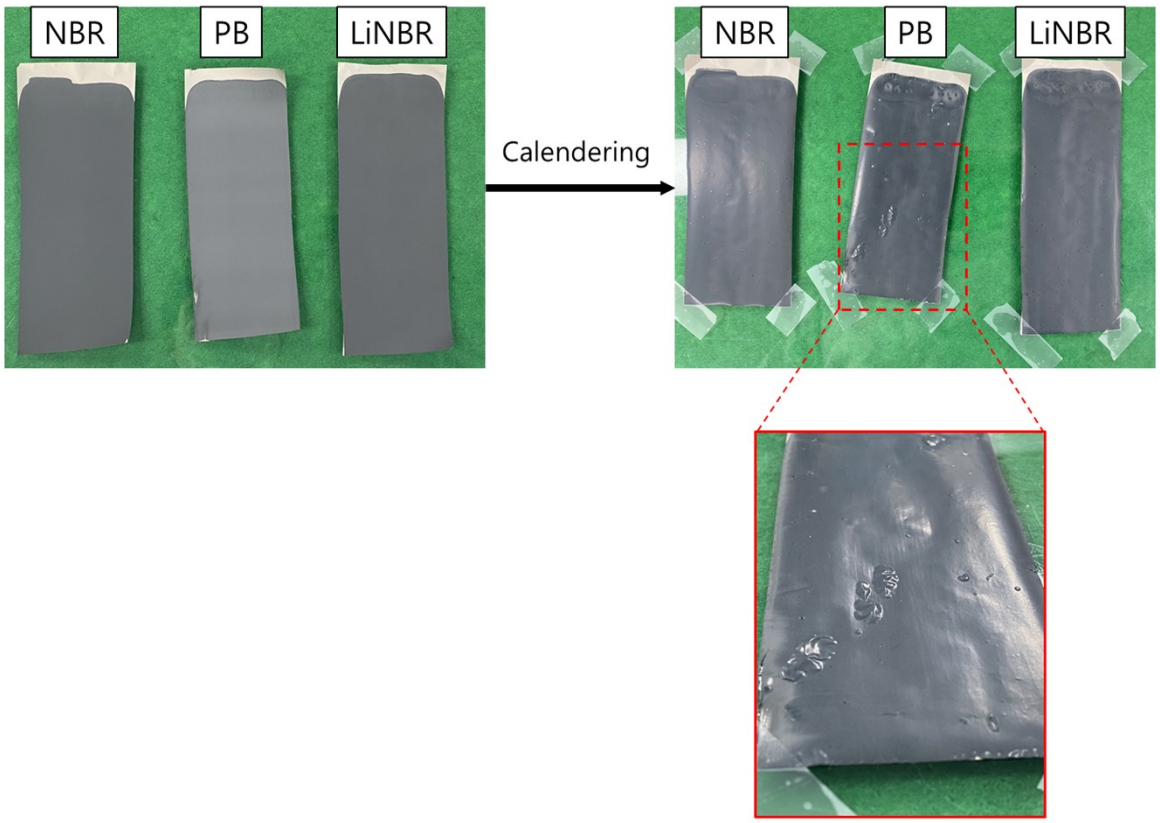

Figure S25. Photographs of LCO composite electrode fabricated with different binder materials before and after calendering process.

Table S1. Summary of the initial charge-discharge results from each binder system (tests conducted with more than three independent samples of each type).

	Charge cap. (mAh g^{-1})	**Discharge cap. (mAh g^{-1})**	**Coulombic efficiency (%)**
NBR	152.5 (± 1.7)	121.3 (± 2.7)	79.6 (± 1.1)
NBR9PB1	149.4 (± 1.5)	119.8 (± 0.9)	80.2 (± 0.4)
NBR5PB5	148.3 (± 4.2)	120.7 (± 3.3)	81.4 (± 0.8)
PB	142.9 (± 4.1)	125.4 (± 3.4)	87.8 (± 0.5)

Table S2. Calculation of the signal area of each component obtained in S 2p spectra for pristine and after 100 cycled LCO composite electrodes (NBR binder vs. PB binder).

Sample	Condition	Components (S 2p)		Total
		PS_4^{3-}	Bridging S	
NBR	Pristine	1.00	-	1.00
	After 100 cycles	0.71	0.29	1.00
PB	Pristine	1.00	-	1.00
	After 100 cycles	0.81	0.19	1.00

Table S3. Calculation of the signal area of each component obtained in P 2p spectra for pristine and after 100 cycled LCO composite electrodes (NBR binder vs. PB binder).

Sample	Condition	Components (P 2p)		Total
		PS_4^{3-}	Bridging S	
NBR	Pristine	1.00	-	1.00
	After 100 cycles	0.34	0.66	1.00
PB	Pristine	1.00	-	1.00
	After 100 cycles	0.63	0.37	1.00

Table S4. Summary of the initial charge-discharge results from each binder system (tests conducted with more than three independent samples of each type).

	Charge cap. (mAh g^{-1})	**Discharge cap. (mAh g^{-1})**	**Coulombic efficiency (%)**
NBR	152.5 (± 1.7)	121.3 (± 2.7)	79.6 (± 1.1)
PB	142.9 (± 4.1)	125.4 (± 3.4)	87.8 (± 0.5)
LiNBR-0.5	148.3 (± 4.2)	120.7 (± 3.3)	89.2 (± 1.5)

Table S5. Calculation of the signal area of each component obtained in S 2p spectra for pristine and after 100 cycled LCO composite electrodes (NBR binder vs. LiNBR-0.5 binder).

Sample	Condition	Components (S 2p)		Total
		PS_4^{3-}	Bridging S	
NBR	Pristine	1.00	-	1.00
	After 100 cycles	0.71	0.29	1.00
LiNBR-0.5	Pristine	1.00	-	1.00
	After 100 cycles	0.74	0.26	1.00

Table S6. Calculation of the signal area of each component obtained in P 2p spectra for pristine and after 100 cycled LCO composite electrodes (NBR binder vs. LiNBR-0.5 binder).

Sample	Condition	Components (P 2p)		Total
		PS_4^{3-}	Bridging S	
NBR	Pristine	1.00	-	1.00
	After 100 cycles	0.34	0.66	1.00
LiNBR-0.5	Pristine	1.00	-	1.00
	After 100 cycles	0.52	0.48	1.00